ELSEVIER

Journal of Molecular Structure 550–551 (2000) 521–530

Journal of
MOLECULAR
STRUCTURE

www.elsevier.nl/locate/molstruc

# Raman, infrared, and microwave spectra and conformational preferences of *meso*-Bisoxirane[☆,☆☆]

V.F. Kalasinsky[a,*], S. Subramaniam[b], C.-F. Su[c], R.L. Cook[c]

[a]*Department of Environmental and Toxicologic Pathology, Armed Forces Institute of Pathology, Washington, DC 20306, USA*
[b]*Department of Chemistry, Mississippi State University, Mississippi, MS 39762, USA*
[c]*Department of Physics and Astronomy, Mississippi State University, Mississippi, MS 39762, USA*

Received 1 December 1999; accepted 8 February 2000

**Abstract**

Vibrational infrared and Raman spectra of liquid and solid *meso*-bisoxirane and infrared spectra of the gaseous phase were recorded. Additionally, microwave rotational spectra from 40 to 18 GHz were recorded. The vibrational spectra demonstrate the presence of two conformations in the fluid phases but only one in the solid state. Infrared and Raman activities and gas-phase band contours indicate that the *trans* conformer with $C_i$ molecular symmetry is more stable than the *gauche* conformer ($C_1$ symmetry). Variable temperature studies of two pairs of Raman lines are consistent with a $\Delta H$ value of $0.31 \pm 0.10$ kcal/mol in the liquid state. Rotational constants ($A = 9187.45 \pm 0.04$, $B = 2651.80 \pm 0.01$, $C = 2608.92 \pm 0.01$ MHz) and the dipole moment ($\mu_{\text{total}} = 3.03$ D) were determined for the *gauche* conformer. Model calculations give an acceptable match to the observed rotational constants for an H–C–C′–H′ dihedral angle of 60°. The relationship of *meso*-bisoxirane to other similar three-membered ring compounds is discussed. Published by Elsevier Science B.V.

*Keywords*: *meso*-Bisoxirane; Raman, infrared and microwave spectra; Coformational preferences

## 1. Introduction

*meso*-Bisoxirane is a structural analog of bicyclopropyl (Fig. 1), with an oxygen atom substituted for one of the carbons on each three membered ring. *d*,*l*-Bisoxirane is its structural isomer, and both these compounds have been shown to possess carcinogenic activity [1,2]. An extensive study on *d*,*l*-bisoxirane has been reported by Su et al. [3] in which rotational constants, possible conformers and a vibrational analysis of this molecule were discussed. The molecule was shown to exist in predominantly two conformers in the liquid and gaseous states. In the solid state, it was found to exist in the more stable nearly *trans* conformer with an HC–H′C′ dihedral angle near 190°. In the liquid phase, the nearly *trans* conformer was found to be more stable than a nearly *gauche* conformer (HC–C′H′ ~40–50°) by $0.23 \pm 0.08$ kcal/mol. Rotational constants and dipole moment for the nearly *trans* conformation were determined in the gaseous state using microwave spectroscopy.

Even though *d*,*l*-bisoxirane has been well-characterized, relatively little work has been reported on the

---

[☆] Dedicated to Professor James R. Durig on the occasion of his 65th birthday.

[☆☆] Disclaimer: The opinions and assertions expressed herein are the private views of the authors and are not to be construed as official or as representing the views of the Armed Forces Institute of Pathology, the Department of the Army, or the Department of Defense.

[*] Corresponding author. Tel.: + 1-202-782-2835; fax: + 1-202-782-9215.

0022-2860/00/$ - see front matter Published by Elsevier Science B.V.
PII: S0022-2860(00)00437-3

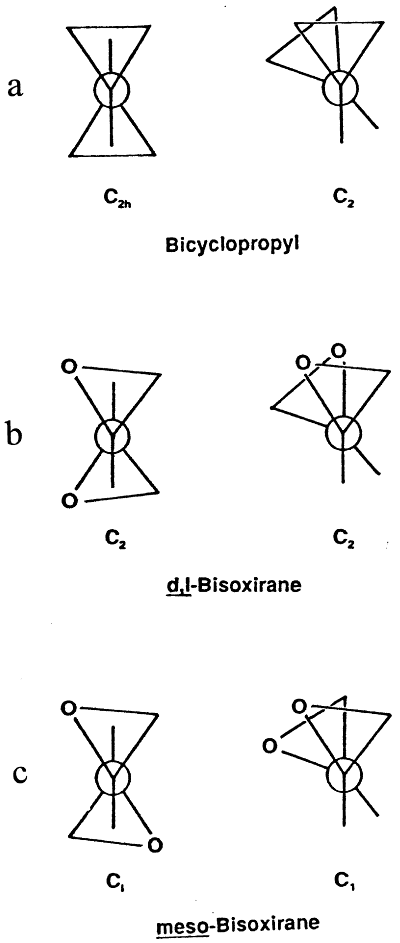

Fig. 1. Conformations of (a) bicyclopropyl, (b) *d,l*-bisoxirane and (c) *meso*-bisoxirane.

isomeric form, *meso*-bisoxirane. The earliest report on *meso*-bisoxirane indicated that two conformers exist in the liquid and gaseous states while only the more stable of these two conformers, which is the trans isomer, was found in the crystalline state [4]. The less stable form was presumed to possess $C_1$ symmetry, and the *trans* isomer possesses $C_i$ point group symmetry. Only the gauche isomer with $C_1$ symmetry can possess a permanent dipole moment and, hence, molecular constants like principal moments and rotational constants may be determined for the *gauche* conformer using microwave spectroscopy. The infrared and Raman spectra of crystalline *meso*-bisoxirane showed mutual exclusion confirming that the *trans* isomer with $C_i$ symmetry exists in the solid state [4].

The measured values of dipole moments and molar Kerr constants for *meso*-bisoxirane in solution [5] in another study suggested that this molecule existed as a mixture of *trans* and *gauche* conformers in solution. A *trans–gauche* equilibrium in which the *trans*:*gauche* ratio is approximately 20:80 was proposed. The reported $HC–C'H'$ dihedral angle of 60° for the *gauche* conformer and the equilibrium ratio of the *gauche* and *trans* conformers in the liquid phase can be confirmed or refuted by using infrared, Raman, and microwave spectroscopic data, but the data for *meso*-bisoxirane are incomplete. Hence, this project was undertaken to carry out a systematic vibrational and rotational assignment and to determine the conformational stability of *meso*-bisoxirane.

## 2. Experimental section

The preparation of *meso*-bisoxirane was carried out in three steps as described in the literature [6]. Reagents were obtained from the Aldrich Chemical Company. *trans*-l,4-Dibromo-2-butene was refluxed with PbO in water to obtain *trans*-l,4-dihydroxy-2-butene. The crude diol was purified by vacuum distillation. The purified *trans*-2-butene-l,4-diol was dissolved in dry ether, and bromine (in dry ether) was added to obtain 1,4-dihydroxy-2,3-dibrombutane. The product was dried under vacuum and recrystallized with alcohol and hexane. Dehydrobromination of 1,4-dihydroxy-2,3-dibromobutane was carried out by using a suspension of KOH in anhydrous ether to produce *meso*-bisoxirane. The product was purified by trap-to-trap distillation with traps cooled to $-76$°C and $-196$°C.

Raman spectra were recorded on a Spex Ramalog DUV spectrometer equipped with a Spectra-Physics Model 171 argon-ion laser operating at 488 nm. Spectra of liquid samples were obtained after sealing the samples in Pyrex capillary tubes, and spectra of samples at low temperatures were recorded using a Raman cell similar to one described by Miller and Harney [7]. Temperatures were monitored with an iron–constantan thermocouple and an Omega Engineering model 199 digital thermometer.

Infrared spectra were obtained between 4000 and

Table 1
Observed Raman and infrared frequencies ($cm^{-1}$) for *meso*-Bisoxirane

| Raman | | Infrared | | | Assignments |
|---|---|---|---|---|---|
| Liquid | Solid | Gas | Liquid | Solid | |
| 3077 m | 3077 m | | | | $CH_2$ antisymmetric stretch |
| | | 3064 R | | | |
| | | 3060 Q,s | 3060 m | 3076 w | $CH_2$ antisymmetric stretch |
| | | 3052 P | | | |
| | 3024 s | | | | C–H stretch |
| 3010 vs | | | | | |
| | 3015 s,sh | | | | $CH_2$ symmetric stretch |
| | | 3012 R | | | |
| | | 3006 Q,s | 3000 s | 3013 s | $CH_2$ symmetric stretch |
| | | 3000 P | | | |
| 1493 m | 1506 w | | | | $CH_2$ deformation |
| | 1500 sh | | | | |
| 1478 sh | | | | | $CH_2$ deformation (*gauche*) |
| | | 1494 R | | | |
| | | 1488 Q | | | |
| | | 1486 Q,w | 1480 m | 1472 m | $CH_2$ deformation |
| | | 1481 P | | | |
| 1449 m | 1451 s | | | | C–H bend |
| 1421 m | | 1425 vw | 1418 m | | C–H bend (*gauche*) |
| 1388 vw | | 1382 Q,w | 1380 w | | C–H bend (*gauche*) |
| | | 1320 R | | 1321 s | |
| | | 1314 Q,m | 1315 m | 1307 s | C–H bend |
| | | 1308 P | | | |
| 1268 s,sh | | 1265 Q | 1263 m | | Ring breathing (*gauche*) |
| 1254 s | 1262 vs | | | | Ring breathing |
| | 1250 vw,sh | | | | |
| | | 1259 R | | | |
| | | | 1250 m | 1252 w | Ring breathing |
| | | 1250 P | | | |
| 1200 vw | 1200 vw | | | | |
| 1188 vw | 1190 vw | | | | $CH_2$ twist |
| | | 1158 Q vvw | | 1159 s | $CH_2$ twist |
| | | | 1150 w | | |
| | | 1148 Q,vvw | | 1138 m | $CH_2$ wag |
| 1141 m | 1146 w | | | | $CH_2$ wag |
| | 1142 sh | | | | |
| 1103 w | | | 1100 vw | | $CH_2$ wag (*gauche*) |
| 1082 w | 1089 vw | | | | C–H bend |
| | | 1077 Q | 1075 vw | 1078 vw | C–H bend |
| 1035 w | | 1031 Q | 1030 w | | C–H bend (*gauche*) |
| | | 1010 R | | | |
| 1005 w | | 1003 Q,w | 1000 w | | C–H bend (*gauche*) |
| | | 995 P | | | |
| | 946 sh | | | | |
| 940 m | 938 m | | | | Ring deformation (asymmetric) |
| | | 939 Q,vvw | 940 w,sh | 943 w | Ring deformation (asymmetric) |
| 915 m | | 925 Q,vw | 910 s | 913 vw | Ring deformation (*gauche*) |
| 876 m | | | | | Ring deformation (*gauche*) |
| | | 888 R | 875 vs | | |
| | | 884 Q,s | 870 vs | 858 vs | Ring deformation (symmetric) |
| | | 876 P | | | |

Table 1 (*continued*)

| Raman | | Infrared | | | Assignments |
|---|---|---|---|---|---|
| Liquid | Solid | Gas | Liquid | Solid | |
| 850 sh | | | 842 sh | | Ring deformation (*gauche*) |
| 830 m | 831 s | | | | Ring deformation (symmetric) |
| 807 m | | | | | $CH_2$ rock (*gauche*) |
| | | 832 R | | | |
| | | 827 Q,m | 802 s | 804 m | $CH_2$ rock |
| | | 822 P | | | |
| | 791 m | | | | $CH_2$ rock |
| 787 m | | | | | |
| | 782 m | | | | C–C stretch |
| | | 746 R | | | |
| 735 w | | 740 Q,s | 730 m | | $CH_2$ rock (*gauche*) |
| | | 733 sh | | | |
| | | 590 R | | | |
| 588 vw | | 584 Q,w | 580 m | | C–C–O bend, out-of-plane (*gauche*) |
| | | 583 Q | | | |
| | | 577 P | | | |
| | 517 sh | | | | |
| 512 w | 513 w | | | | C–C–O bend, out-of-plane |
| | | 470 R | | | |
| 474 w | | 465 Q,vw | 470 m | | C–C–O bend, in-plane (*gauche*) |
| | | 460 P | | | |
| 408 m | 408 s | | | | C–C–O bend, in-plane |
| 258 w | | | | | C–C–O bend, out-of-plane (*gauche*) |
| | 150 vw | | | | Lattice mode |

400 $cm^{-1}$ by using a Nicolet 7199 Fourier transform interferometer equipped with a KBr/Ge beamsplitter and a liquid-nitrogen cooled mercury–cadmium–telluride (MCT) detector. Spectra of the vapor were obtained by placing the sample in a 12-cm, glass-bodied, O-ring cell fitted with KBr windows, while spectra of solid samples were obtained by using a low-temperature cell which was equipped with a cold finger attached to a brass block and cooled with liquid nitrogen. Sample was sprayed onto a KBr window, which was supported on the cold brass block.

The microwave rotational spectral lines presented in this report were measured by using conventional Stark-modulated Hewlett-Packard 8400 or 8460 microwave spectrometers in the X-, K-, and R-band frequency regions. The measurements in the X-band region were used only for the Stark effect studies. The measurements were made at room temperature with a sample pressure of 60 mtorr or less. The frequency measurements are accurate to 0.10 MHz or better. For the Stark effect studies, the Stark cell was calibrated at high electric field with OCS, $\mu = 0.71521$ D, and at low fields with $CF_3CCH$, $\mu = 2.327$ D.

## 3. Results

*Vibrational Assignments*. Each conformer of *meso*-bisoxirane possesses 30 normal vibrations. For the more stable conformer with $C_i$ symmetry, the principle of mutual exclusion applies, so 15 are infrared active and 15 are Raman active. The infrared active $A_u$ vibrations of this conformer will give rise to A-, B-, C-type or hybrid band contours in the infrared spectrum of the gas. All 30 normal vibrations of the *gauche* conformer ($C_1$ symmetry) will be both Raman and infrared active. The assignments of the observed infrared and Raman spectra are shown in

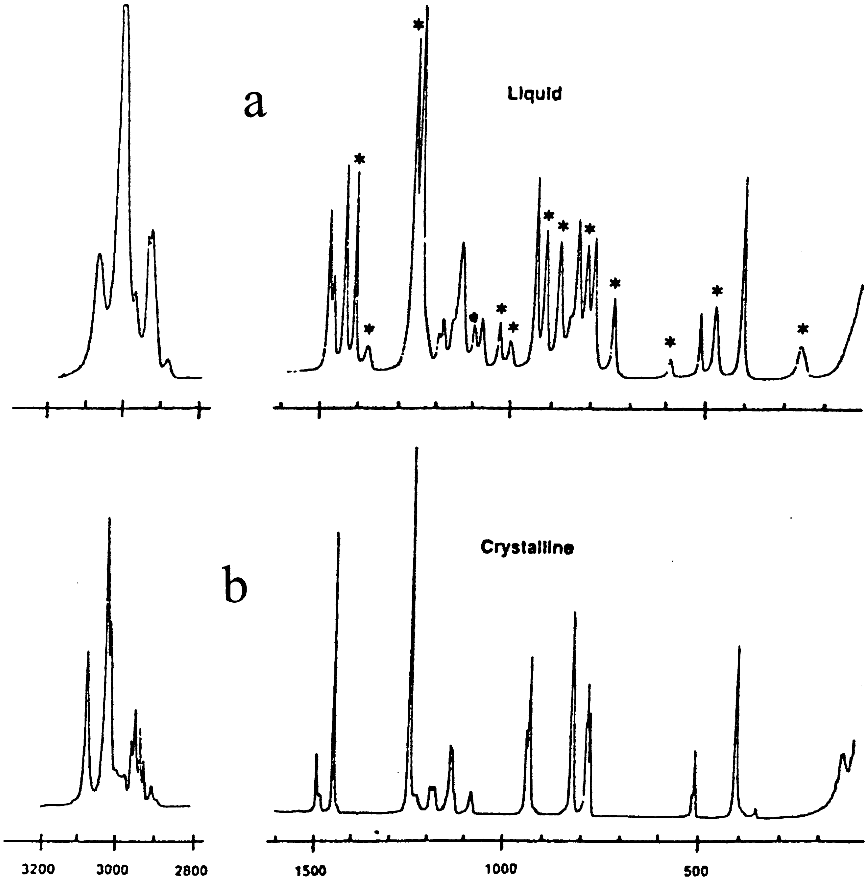

Fig. 2. Raman spectra of (a) liquid *meso*-bisoxirane and (b) crystalline *meso*-bisoxirane. The marks indicate conformational peaks which disappear during the crystallization process.

Table 1 and are consistent with those made for other oxirane derivatives [3,8–11].

The infrared band contours are not particularly helpful in making assignments or distinguishing conformers because of the hybrid contours observed in the spectrum of the vapor. The one exception is the B-type contour, with maxima at 1259 and 1250 cm$^{-1}$, which corresponds to the infrared-active ring breathing mode of *trans-meso*-bisoxirane.

The Raman and infrared spectra of liquid *meso*-bisoxirane show bands corresponding to the two conformers of this molecule. On cooling and subsequent solidification, several of the bands in the spectra of the liquid and amorphous solid disappeared in the crystalline solid (Figs. 2 and 3). The most intense bands in the spectra of the liquid correspond to bands observed for the crystalline solid and are, therefore, assigned to the more stable conformer, while the peaks that disappeared in going from the liquid to the solid were assigned to the less stable conformer. In comparing the Raman and infrared spectra of the crystalline solid, it is clear that the principle of mutual exclusion holds as expected for $C_i$ molecular symmetry in the *trans* conformer [4]. (See Fig. 1.) By contrast, the peaks assigned to the less stable *gauche* conformer are generally coincident in the Raman and infrared spectra as expected for $C_1$ symmetry. Thus the peaks at 1478, 1421 (1418), 1388 (1380), 1268, 1103 (1100), 1035 (1030), 1005 (1000), 915, 876, 850, 807, 735 (730), 588 (580), 474 (470) and 258 cm$^{-1}$ in the Raman (or infrared) spectrum of the liquid state, which are absent from the

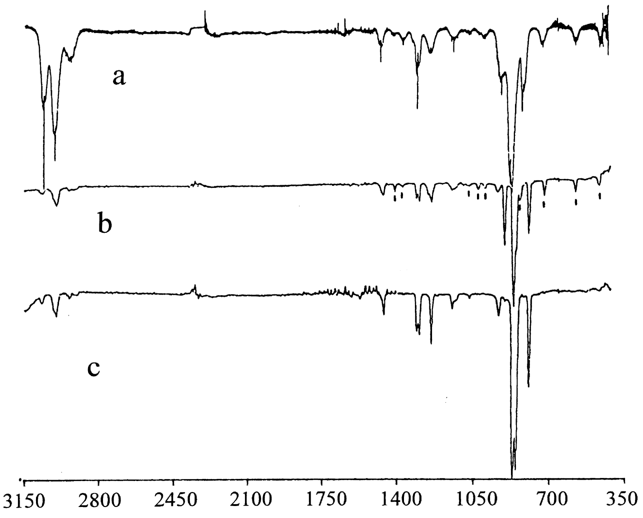

Fig. 3. Infrared spectra of (a) gaseous, (b) amorphous, and (c) crystalline *meso*-bisoxirane in the frequency region between 3150 and 400 $\text{cm}^{-1}$. The marks indicate conformational peaks which disappear during the crystallization process.

spectra of the solid, were attributed to the *gauche* conformer. The very weak feature at 913 $\text{cm}^{-1}$ in the infrared spectrum is probably due to a small number of *gauche* molecules remaining in an incompletely annealed solid. The peaks in the liquid at 1268, 735, 588 and 474 $\text{cm}^{-1}$ were assigned to the ring breathing, $CH_2$ rock, $C'CO$ bend (in-plane, out-of-phase), and $C'CO$ bend (in-plane, in-phase), respectively, for the *gauche* conformer and are candidates for studying the conformational equilibrium.

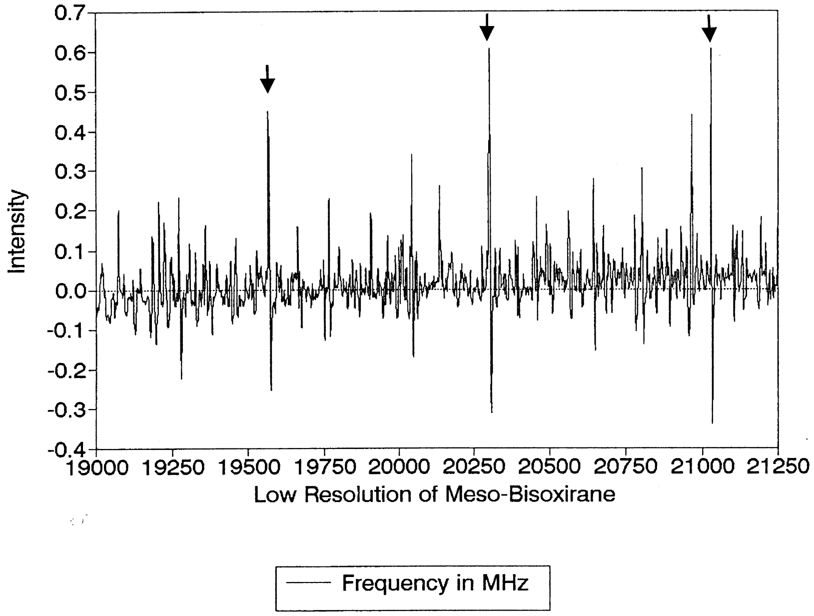

Fig. 4. Microwave spectrum of *meso*-bisoxirane vapor from 21 to 19 GHz.

Table 2
Observed transition frequencies (MHz) of the ground vibrational state of *gauche meso*-Bisoxirane (calculated frequencies are obtained using the spectroscopic constants in Table 3)

| Transition | Observed | Obs.–Cal. | Transition | Observed | Obs.–Cal. |
|---|---|---|---|---|---|
| $2_{21} \leftarrow 1_{11}$ | 30213.54 | 0.07 | $2_{20} \leftarrow 1_{10}$ | 30171.02 | 0.21 |
| $3_{22} \leftarrow 2_{12}$ | 35516.94 | −0.24 | $3_{21} \leftarrow 2_{11}$ | 35389.38 | −0.22 |
| $4_{13} \leftarrow 3_{03}$ | 27814.85 | −0.10 | $5_{14} \leftarrow 4_{04}$ | 33184.18 | 0.03 |
| $6_{06} \leftarrow 5_{05}$ | 31557.42 | 0.30 | $6_{16} \leftarrow 5_{15}$ | 31434.47 | 0.26 |
| $6_{15} \leftarrow 5_{14}$ | 31691.87 | 0.37 | $6_{25} \leftarrow 5_{24}$ | 31564.32 | 0.55 |
| $6_{24} \leftarrow 5_{23}$ | 31571.42 | 0.30 | $6_{15} \leftarrow 5_{05}$ | 38575.99 | −0.17 |
| $7_{07} \leftarrow 6_{06}$ | 36183.44 | −0.08 | $7_{17} \leftarrow 6_{16}$ | 36672.32 | −0.02 |
| $7_{16} \leftarrow 6_{15}$ | 36972.66 | −0.02 | $7_{26} \leftarrow 6_{25}$ | 36823.79 | −0.14 |
| $7_{25} \leftarrow 6_{24}$ | 36835.57 | −0.13 | $7_{07} \leftarrow 6_{15}$ | 29794.27 | −0.21 |
| $8_{35} \leftarrow 8_{27}$ | 32796.60 | 0.17 | $8_{36} \leftarrow 8_{26}$ | 32752.12 | 0.10 |
| $8_{08} \leftarrow 7_{16}$ | 34890.00 | −0.31 | $9_{36} \leftarrow 9_{28}$ | 32304.52 | 0.20 |
| $9_{37} \leftarrow 9_{27}$ | 32734.41 | −0.05 | $9_{09} \leftarrow 8_{17}$ | 39958.70 | 0.05 |
| $9_{19} \leftarrow 8_{27}$ | 26700.03 | −0.37 | $9_{18} \leftarrow 8_{26}$ | 28585.59 | −0.17 |
| $10_{37} \leftarrow 10_{29}$ | 32815.29 | 0.16 | $10_{38} \leftarrow 10_{28}$ | 32710.04 | −0.19 |
| $11_{38} \leftarrow 11_{2,10}$ | 32829.63 | 0.10 | $11_{39} \leftarrow 11_{29}$ | 32677.81 | −0.06 |
| $11_{1,11} \leftarrow 10_{29}$ | 36761.06 | −0.14 | $11_{1,10} \leftarrow 10_{28}$ | 39487.18 | 0.46 |
| $12_{39} \leftarrow 12_{2,11}$ | 32848.26 | 0.01 | $12_{3\ 10} \leftarrow 12_{2,10}$ | 32635.69 | −0.11 |
| $13_{3,10} \leftarrow 13_{2,12}$ | 32872.20 | 0.06 | $13_{3,11} \leftarrow 13_{2,11}$ | 32582.33 | −0.01 |
| $14_{3,11} \leftarrow 14_{2,13}$ | 32902.15 | 0.03 | $14_{3,12} \leftarrow 14_{2,12}$ | 32515.77 | 0.17 |
| $15_{3,12} \leftarrow 15_{2,14}$ | 32939.22 | 0.03 | $15_{3,13} \leftarrow 15_{2,13}$ | 32434.13 | −0.06 |
| $16_{3,13} \leftarrow 16_{2,15}$ | 32984.45 | −0.02 | $16_{3,14} \leftarrow 16_{2,14}$ | 32335.76 | −0.09 |
| $17_{3,14} \leftarrow 17_{2,16}$ | 33039.09 | 0.08 | $17_{3,15} \leftarrow 17_{2,15}$ | 32218.91 | 0.00 |
| $18_{3,15} \leftarrow 18_{2,17}$ | 33104.61 | 0.00 | $18_{3,16} \leftarrow 18_{2,16}$ | 32081.54 | −0.05 |
| $19_{3,16} \leftarrow 19_{2,18}$ | 33182.19 | −0.01 | $19_{3,17} \leftarrow 19_{2,17}$ | 31922.14 | −0.06 |
| $20_{3,17} \leftarrow 20_{2,19}$ | 33273.50 | −0.01 | $20_{3,18} \leftarrow 20_{2,18}$ | 31739.02 | −0.17 |
| $21_{3,18} \leftarrow 21_{2,20}$ | 33380.17 | 0.01 | $21_{3,19} \leftarrow 21_{2,19}$ | 31531.09 | −0.04 |
| $22_{2,20} \leftarrow 22_{1,22}$ | 27344.89 | −0.18 | $22_{3,19} \leftarrow 22_{2,21}$ | 33504.06 | 0.05 |
| $22_{3,20} \leftarrow 22_{2,20}$ | 31296.80 | 0.01 | $23_{2,21} \leftarrow 23_{1,23}$ | 28232.24 | −0.05 |
| $23_{3,20} \leftarrow 23_{2,22}$ | 33646.91 | 0.03 | $23_{3,21} \leftarrow 23_{2,21}$ | 31035.21 | 0.34 |
| $24_{2,22} \leftarrow 24_{1,24}$ | 39183.94 | −0.05 | $24_{3,21} \leftarrow 24_{2,23}$ | 33810.96 | 0.03 |
| $24_{3,22} \leftarrow 24_{2,22}$ | 30745.54 | 0.07 | $25_{3,23} \leftarrow 25_{2,23}$ | 30427.24 | 0.20 |
| $25_{3,22} \leftarrow 25_{2,24}$ | 33998.28 | 0.03 | $25_{2,23} \leftarrow 25_{1,25}$ | 30201.57 | 0.14 |
| $26_{3,23} \leftarrow 26_{2,25}$ | 34211.20 | 0.02 | $27_{3,24} \leftarrow 27_{2,26}$ | 34452.10 | −0.05 |
| $27_{3,25} \leftarrow 27_{2,25}$ | 39703.28 | −0.12 | $28_{3,25} \leftarrow 28_{2,27}$ | 34723.74 | −0.01 |
| $28_{3,26} \leftarrow 28_{2,26}$ | 29297.94 | −0.11 | $29_{3,26} \leftarrow 29_{2,28}$ | 35028.54 | −0.06 |
| $29_{3,27} \leftarrow 29_{2,27}$ | 28864.03 | −0.05 | $30_{3,27} \leftarrow 30_{2,29}$ | 35369.46 | −0.08 |
| $30_{3,28} \leftarrow 30_{2,23}$ | 28401.96 | −0.03 | $31_{3,28} \leftarrow 31_{2,30}$ | 35749.42 | −0.01 |
| $31_{3,29} \leftarrow 31_{2,29}$ | 27912.48 | 0.01 | $32_{3,29} \leftarrow 32_{2,31}$ | 36171.20 | −0.03 |
| $32_{3,30} \leftarrow 32_{2,30}$ | 27396.30 | −0.04 | $33_{3,30} \leftarrow 33_{2,32}$ | 36637.88 | −0.05 |
| $33_{3,31} \leftarrow 33_{2,31}$ | 26854.59 | 0.03 | $34_{3,31} \leftarrow 34_{2,33}$ | 37152.50 | −0.06 |
| $34_{3,32} \leftarrow 34_{2,34}$ | 26288.27 | −0.07 | $35_{3,32} \leftarrow 35_{2,34}$ | 37718.12 | −0.04 |
| $35_{3,33} \leftarrow 35_{2,33}$ | 25698.42 | −0.01 | $36_{3,33} \leftarrow 36_{2,35}$ | 38337.68 | −0.20 |
| $36_{3,34} \leftarrow 36_{2,34}$ | 25086.50 | 0.01 | $37_{3,34} \leftarrow 37_{2,36}$ | 39014.22 | −0.12 |
| $37_{3,35} \leftarrow 37_{2,35}$ | 24453.87 | −0.14 | $38_{3,36} \leftarrow 38_{2,36}$ | 23801.60 | −0.04 |
| $38_{3,35} \leftarrow 38_{2,37}$ | 39750.26 | 0.11 | $39_{3,37} \leftarrow 39_{2,37}$ | 23131.47 | 0.03 |
| $40_{3,38} \leftarrow 40_{2,38}$ | 22445.00 | 0.09 | $41_{3,39} \leftarrow 41_{2,39}$ | 21743.54 | −0.05 |
| $42_{3,40} \leftarrow 42_{2,40}$ | 21029.21 | 0.06 | $43_{3,41} \leftarrow 43_{2,41}$ | 20303.28 | −0.03 |
| $44_{3,42} \leftarrow 44_{2,42}$ | 19567.87 | −0.03 | $45_{3,43} \leftarrow 45_{2,43}$ | 18824.75 | −0.03 |
| $46_{3,44} \leftarrow 46_{2,44}$ | 18075.86 | −0.04 |  |  |  |

In the solid state, some of the bands for the *trans* conformer exhibit splitting probably due to the presence of two or more molecules per unit cell in the crystalline solid. The pairs of bands in the infrared spectrum at 1320 and 1310 $\text{cm}^{-1}$ and 875 and 858 $\text{cm}^{-1}$, for the C–H bend and a ring deformation, respectively, are examples. Similarly the peaks at 1200 and 1190 $\text{cm}^{-1}$ and at 517 and 513 $\text{cm}^{-1}$, assigned to the $CH_2$ rock and C′–C–O bend, are observed in the Raman spectrum. Another pair of Raman lines, at 791 and 782 $\text{cm}^{-1}$, might reflect crystal splitting or two different fundamental vibrations as indicated in Table 1, but it is impossible to be certain.

*Conformer Stability*. The changes in intensity of the pairs of conformer peaks at 474 and 408 $\text{cm}^{-1}$ and at 588 and 512 $\text{cm}^{-1}$ in the Raman spectrum of the liquid were monitored over a temperature range from 297K to 247K. These pairs showed changes in peak area with changes in temperature. The van't Hoff equation for the determination of $\Delta H$ is given by:

$$\ln(I/I') = -(\Delta H/R)(1/T) + \text{const.}$$

Using the intensity ratios and absolute temperatures, plots of reciprocal temperature versus the natural logarithm of intensity ratios for the aforementioned peak pairs were prepared. The slopes ($\Delta H/R$) of the least-squares straight lines were 142.1 ± 20.9 K and 172.7 ± 47.3 K for the lower- and higher-frequency peak pairs, respectively. The average $\Delta H$ value was found to be 0.31 ± 0.10 kcal/mol.

*Microwave spectra*. The structural parameters used for *d*,*l*-bisoxirane were used to predict the rotational spectrum of *meso*-bisoxirane, and the dipole moment of ethylene oxide was used to estimate its dipole moment components. Because of symmetry, the dipole moment components were found to be zero in the *trans* form. Those of the *gauche* form, on the other hand, were found to be substantial. Hence, the rotational spectrum of the *gauche* form is expected in the observations. Calculations indicate the *gauche* form is a nearly prolate asymmetric rotor with $\kappa = -0.987$.

The calculated moments of inertia along with the estimated dipole moment components indicate that the c-type transitions would be the strongest and the b-type ones the weakest. The predicted rotational spectrum also indicated that a series of high-J Q-branch transitions ($J_{3,J-2} \leftarrow J_{2,J-2}$) would dominate in the K-band frequency region and that the spacing between two adjacent lines would increase very slightly as the frequency decreases and the rotational quantum number increases. A portion of the recorded low-resolution spectrum in K-band is shown in Fig. 4. It is obvious that a number of strong lines marked with arrows appear with approximately even spacings. Preliminary analysis provided an assignment of the thirteen lines observed in the K-band frequency region for the rotational quantum numbers from 34 to 46. Analysis of these lines gave an improved set of rotational constants. Transitions of the same series at higher frequency and transitions of another series ($J_{3,J-3} \leftarrow J_{2,J-1}$) were predicted, and these lines were measured and added to the analysis.

The observed Q-branch transitions could only be used to determine two rotational parameters. R-branch transition lines were needed to evaluate the three rotational constants. The predicted spectrum showed that two series of c-type, low-J, R-branch transitions were in the K- and R-band frequency regions. The series are $J_{0,J} \leftarrow (J-1)_{1,J-2}$ and $J_{1,J-1} \leftarrow (J-1)_{0,J-1}$. In each of the series, the spacing between two adjacent lines was approximately B + C. Additionally, the Stark behavior of the transition lines for each series was expected to be similar. After some searching, four lines of each series were assigned and used to predict other transitions.

Besides the c-type transitions, the weaker a- and b-type R-branch transitions were also assigned and included in the analysis. The 97 assigned lines listed in Table 2 were used to evaluate the spectroscopic constants. An effective rotational Hamiltonian including the effects of centrifugal distortion was employed [12]. The evaluated constants are listed in Table 3. The spectral lines were fit with a standard deviation of 0.15 MHz using these constants.

Due to a dense spectrum, only three rotational transitions listed in Table 2 were studied for the Stark effect analysis. The Stark effect was found to be second order. The Stark splittings and necessary parameters were used to determine the dipole moment components by a least-squares fit method. The evaluated values are also listed in Table 4.

The structural parameters initially used to predict the rotational transitions were adjusted slightly to

Table 3
Spectroscopic constants (in MHz) for the ground vibrational state of *gauche meso*-Bisoxirane

$A = 9187.45 \pm 0.04$
$B = 2651.80 \pm 0.01$
$C = 2608.92 \pm 0.01$
$\Delta_J = (-0.182 \pm 0.047) \times 10^{-3}$
$\Delta_K = (-0.533 \pm 0.00011) \times 10^{-1}$
$\Delta_{JK} = (-0.496 \pm 0.304) \times 10^{-2}$
$\delta_J = (-0.441 \pm 0.0012) \times 10^{-4}$
$\delta_K = (-0.175 \pm 0.101) \times 10^{-3}$

Table 4
Dipole moment components of the ground vibrational state of *gauche meso*-Bisoxirane

$\mu_a = 1.084 \pm 0.024\,D$
$\mu_b = 0.350 \pm 0.128\,D$
$\mu_c = 2.808 \pm 0.049\,D$
$\mu = 3.030 \pm 0.139\,D$

| Transition | \|M\| |
|---|---|
| $3_{12} \leftarrow 2_{02}$ | 2 |
| $3_{12} \leftarrow 2_{02}$ | 1 |
| $2_{02} \leftarrow 1_{01}$ | 1 |
| $5_{05} \leftarrow 4_{13}$ | 1 |

obtain a better agreement with the experimental rotational constants. These are shown in Fig. 5. Several assumed parameters were used. They are: $\angle$HCH = 120°, $\angle'$HCC$'$ 116°, C–H = 1.09 Å, and $\angle$HCC$'$H$'$ (dihedral angle) = 65.5°. The rotational constants based upon these structural parameters are (in MHz) $A = 9173$, $B = 2666$, and $C = 2605$. These predicted rotational constants are very consistent with those listed in Table 3.

## 4. Discussion

*meso*-Bisoxirane is known to exist as two different conformers. Both the *gauche* and *trans* conformers have been found to exist in the liquid and gaseous states. In the crystalline solid state, the more stable *trans* conformer with $C_i$ symmetry is the only conformer present. *d*,*l*-Bisoxirane, which is a structural isomer of *meso*-bisoxirane, has been shown by infrared and Raman studies to exist in a nearly *trans* conformer and at least one nearly gauche form. The dihedral angles (defined as the angle between the C–H bonds of the two rings) for these two conformers in *d*,*l*-bisoxirane were estimated to be 190 and 45°, respectively. However, the *trans* conformer of *meso*-bisoxirane is presumed to possess a dihedral angle of 180° based on the molecular symmetry ($C_i$) determined from the vibrational spectra and the lack of a microwave spectrum, which implies a zero dipole moment. The *gauche* conformer of *meso*-bisoxirane, which exhibits the observed microwave spectrum, was determined to possess a dihedral angle of approximately 60°. The derived rotational constants

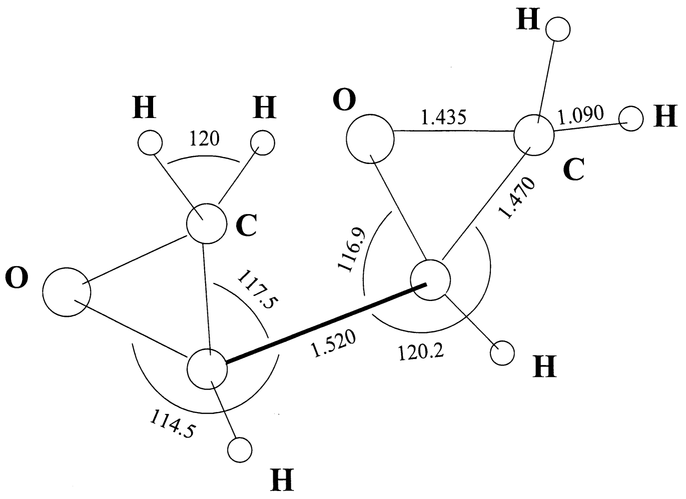

Fig. 5. Assumed structure of *gauche-meso*-bisoxirane.

and dipole moments consistent with this structure are shown in Tables 3 and 4.

Two conformers of *meso-bisoxirane* have been confirmed by the present study, and vibrational bands corresponding to the more stable *trans* conformer were found to be present in the solid state. The peaks corresponding to the $CC'O'$ bends of the *gauche* and *trans* conformers were monitored in a variable temperature study of the liquid phase. It was found that the *trans* conformer is more stable than the *gauche* conformer ($HC–C'H'$ 60°) by 0.31 ± 0.10 kcal/mol. The corresponding enthalpy difference for these conformer pairs is 0.23 ± 0.08 kcal/mol in *d*,*l*-bisoxirane [3].

Two conformers were considered in a study of the solution polarizability of *meso*-bisoxirane [5]. Based on the measured polarizability and molar Kerr constants, the more abundant solution-state confomer for *meso*-bisoxirane was predicted to be the *gauche* conformer with the $HC–C'H'$ dihedral angle of 60°. The dihedral angle inferred in the present study was found to be close to 60° for the *gauche* conformer based on the microwave and infrared data, but the *gauche* conformer is less stable than the *trans*. The $\Delta H$ value for the liquid is small enough, though, that the degeneracy of the *gauche* conformer might make it the more abundant conformer.

Assumed structural parameters taken from *d*,*l*-bisoxirane [3] were used to calculate distances between nonbonded atoms for *meso*-bisoxirane as a function of dihedral angle. If van der Waals radii [13] of 1.7, 1.2, and 1.5 Å for carbon, hydrogen, and oxygen, respectively, are utilized, the only calculated non-bonded distance which is less than the sum of the appropriate radii is the $C'\cdots O$ distance in *gauche* *meso*-bisoxirane. These calculations are consistent with the data which favor a *trans* conformer for *meso*-bisoxirane, but this unfavorable interaction for the *gauche* form can be minimized if the $C'–C–O$ angle (or the tilt between the oxirane rings) is slightly larger than originally assumed. From the diagrams in Fig. 1, it is apparent that the dihedral angle is an important factor in determining the non-bonded $C'\cdots O$ and $O'\cdots O$ distances. In *meso*-bisoxirane, a dihedral angle of the order of 60° satisfactorily achieves this balance, while a smaller dihedral angle (40–50°) is necessary for *d*,*l*-bisoxirane as indicated previously [3].

## References

[1] B.L. Van Dauren, L. Langseth, B.M. Goldschmidt, L. Orris, J. Natl. Cancer Inst. 39 (1967) 1217.
[2] L. Otvos, I. Elekes, Tetrahedron Lett. (1975) 2481.
[3] C.F. Su, R.L. Cook, C. Saiwan, J.A.S. Smith, V.F. Kalasinsky, J. Mol. Spectrosc. 127 (1988) 337.
[4] W. Luttke, A. Demeijere, Tetrahedron Lett. (1966) 4149.
[5] M.J. Aroney, K.E. Calderbank, H.J. Stootman, Aust. J. Chem. 27 (1974) 3194.
[6] W.F. Beech, J. Chem. Soc. (London) (1951) 2483.
[7] F.A. Miller, B.M. Harney, Appl. Spectrosc. 24 (1971) 291.
[8] V.F. Kalasinsky, C.J. Wurrey, J. Raman Spectrosc. 9 (1980) 45.
[9] V.F. Kalasinsky, C.J. Wurrey, J. Raman Spectrosc. 9 (1980) 315.
[10] C.J. Wurrey, R. Krishnamoorthi, S. Pechsiri, V.F. Kalasinsky, J. Raman Spectrosc. 12 (1982) 95.
[11] C.J. Wurrey, Y.Y. Yeh, R. Krishnamoorthi, R.J. Berry, J.E. DeWitt, V.F. Kalasinsky, J. Phys. Chem. 88 (1984) 4059.
[12] W. Gordy, R.L. Cook, Microwave Molecular Spectra, 3, Wiley, New York, 1984.
[13] B.E. Douglas, D.H. McDaniel, J.J. Alexander, Concepts and Models of Inorganic Chemistry, 2, Wiley, New York, 1983.